

# A 3D Facial Reconstruction Evaluation Methodology: Comparing Smartphone Scans with Deep Learning Based Methods Using Geometry and Morphometry Criteria

Álvaro Heredia-Lidón<sup>1</sup>✉, Alejandro Moñux-Bernal<sup>1</sup>, Alejandro González<sup>1</sup>,  
Luis M. Echeverry-Quiceno<sup>2</sup>, Max Rubert<sup>2</sup>, Aroa Casado<sup>2</sup>, María Esther  
Esteban<sup>2</sup>, Mireia Andreu-Montoriol<sup>2</sup>, Susanna Gallardo<sup>2</sup>, Cristina Ruffo<sup>2</sup>,  
Neus Martínez-Abadías<sup>2</sup>, and Xavier Sevillano<sup>1</sup>

<sup>1</sup> HER, La Salle - Universitat Ramon Llull, Barcelona, Spain  
alvaro.heredia@salle.url.edu

<sup>2</sup> BEECA, Facultat de Biologia, Universitat de Barcelona, Barcelona, Spain

**Abstract.** Three-dimensional (3D) facial shape analysis has gained interest due to its potential clinical applications. However, the high cost of advanced 3D facial acquisition systems limits their widespread use, driving the development of low-cost acquisition and reconstruction methods. This study introduces a novel evaluation methodology that goes beyond traditional geometry-based benchmarks by integrating morphometric shape analysis techniques, providing a statistical framework for assessing facial morphology preservation. As a case study, we compare smartphone-based 3D scans with state-of-the-art deep learning reconstruction methods from 2D images, using high-end stereophotogrammetry models as ground truth. This methodology enables a quantitative assessment of global and local shape differences, offering a biologically meaningful validation approach for low-cost 3D facial acquisition and reconstruction techniques.

**Keywords:** Methodology · Facial Shape Analysis · Geometric Morphometrics · Deep Learning-Based Reconstruction.

## 1 Introduction

Three-dimensional (3D) facial model acquisition has been a breakthrough in fields such as plastic surgery [1], orthodontic diagnosis [2] or the study of facial morphology for diagnostic purposes [3]. The potential of these techniques lies in their non-invasive nature, capturing precise details of the face, and resolving the limitations of two-dimensional (2D) analysis.

Acquiring highly accurate 3D facial models usually requires specialised equipment [4]. Examples include stereophotogrammetry systems (SPG) –consisting of multiple cameras capturing images synchronously [5]–, portable devices based on laser technology [6], structural light-based cameras [7] or medical devices

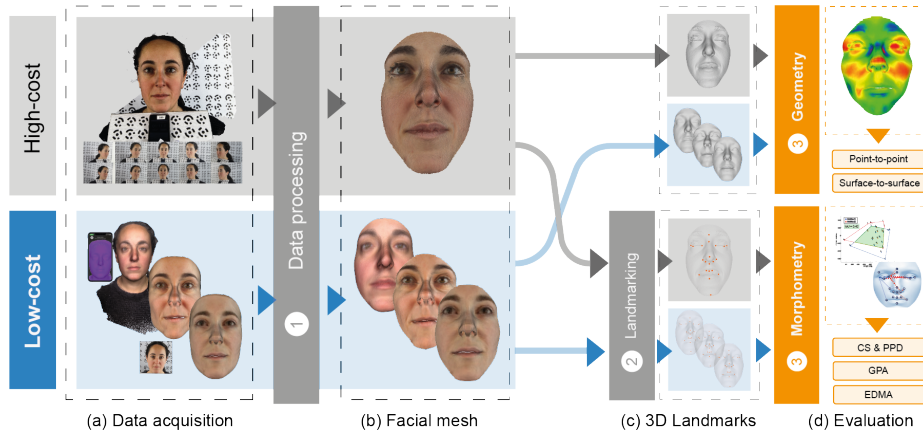


**Fig. 1.** Methodology pipeline. (a) Data acquisition using high-cost 3D stereophotogrammetry system, and low-cost approaches. (b) Facial mesh extraction and normalisation. (c) 3D anatomical landmarks registration for morphometric analysis. (d) Methods comparison based on geometry and morphometry metrics.

like magnetic resonance image scanners [8]. While these techniques yield high-resolution 3D facial reconstructions, they are often expensive and inaccessible, limiting their widespread application in clinical settings [9].

As an alternative, portable structured-light scanners embedded in consumer devices like smartphones have emerged as a promising approach to low-cost 3D facial model acquisition [10,18]. Several studies have validated the applicability of the iPhone’s TrueDepth camera as a viable alternative to high-cost scanners for clinical applications [10,20].

A different low-cost approach consists in deep learning-based methods for reconstructing 3D facial models from a single or multiple 2D images. On the one hand, single-view 3D facial reconstruction has been a long-standing challenge in computer vision, leading to the development of various state-of-the-art approaches. For instance, Lei *et al.* [11] introduced a Hierarchical Representation Network (HRN) that decouples facial geometry to enhance high-fidelity detail reconstruction. Deng *et al.* [12] proposed a weakly-supervised CNN for 3D face reconstruction, while Wang *et al.* [13] leveraged geometric information from facial part silhouettes to guide the reconstruction process, improving structural accuracy.

On the other hand, multi-view methods emerge as a powerful alternative, offering more accurate modelling but relying on camera calibrations and poses [11,14]. Ramon *et al.* [14] presented H3D-Net architecture for high-quality 3D human heads reconstruction from a few input images. Lei *et al.* [11] took advantage of the hierarchical structure of HRN to adapt it to multiple images, adding geometric consistency between different views. Another multi-view approach is diffusion modelling, generating multiple views from a single 2D image,

like in Era3D [15], for subsequent reconstruction of 3D models using NeuS [16] or Gaussian Splatting [17] techniques.

The validation of low-cost 3D facial acquisition and reconstruction methods has predominantly relied on benchmarks such as REALY [21] or NoW [22], which assess geometric accuracy using high-resolution 3D facial models as ground truth [11]. However, these benchmarks are limited to surface-based geometric deviations and fail to account for facial morphology and anatomical consistency. To address this gap, it is necessary to incorporate statistical shape analysis techniques that evaluate the morphological fidelity of reconstructed faces, providing a more anatomically relevant validation framework.

In this context, Geometric Morphometrics (GM) is a robust set of statistical tools that measure the shape of biological structures from the coordinates of a set of anatomical landmarks [23]. The main advantage of GM is that the 3D shape and geometry are preserved throughout the analysis, providing more robust and precise results, detecting subtle shape differences, and allowing the visualization of the results as shape changes [23]. Among the two most commonly used GM techniques in facial analysis are: *i*) Generalized Procrustes Analysis (GPA) [23] to assess global differences in facial shape, and *ii*) Euclidean Distance Matrix Analysis (EDMA) [24] to detect local differences in facial shape.

For this reason, we propose a new evaluation methodology for low-cost 3D facial acquisition and reconstruction methods, which extends beyond traditional geometric assessments by incorporating GM-based metrics (Figure 1). To test our methodology, we compared smartphone-based 3D scans with 2D image-based deep learning 3D reconstruction methods using high-resolution stereophotogrammetry models as ground truth. The results showed that smartphone scans achieved higher geometric and morphometric similarity with respect to the ground truth.

## 2 Materials and Methods

### 2.1 Participants Recruitment and Ethical Statement

A total of 82 volunteers (40 females and 42 males, ages  $30.48 \pm 12.13$ ) with no pathological facial dysmorphologies were recruited. Each individual was captured on the same day by the different acquisition methods. No discriminatory criteria, such as excessive wrinkles or beard, were selected. To guarantee unobstructed facial shape acquisition, participants were asked to remove any hair covering their face and any artefacts such as earrings or piercings when possible, while maintaining a neutral facial expression. All the participants signed an informed consent approved by the Bioethics Committee of Universitat de Barcelona (IRB03099).

### 2.2 Face Acquisition and Reconstruction

The first step of the proposed methodology requires using a high cost acquisition method to obtain the ground truth facial models, and a set of methods to be

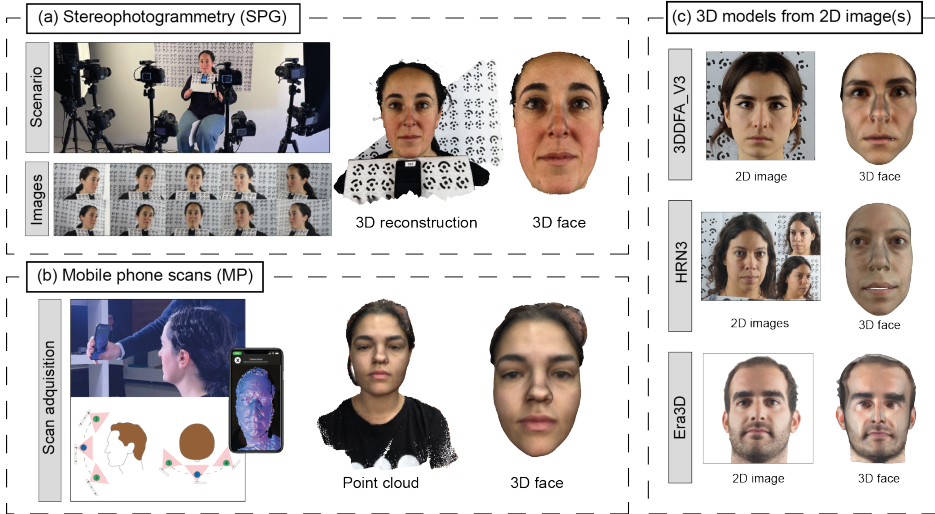


**Fig. 2.** Face acquisition and reconstruction. (a) High quality facial models acquired by a stereophotogrammetry (SPG) system: setup and reconstruction of the 3D facial model from 10 images. (b) Low-cost facial model acquisition via iPhoneX TrueDepth camera and processed 3D model. (c) Low-cost facial reconstruction from 2D image(s): 3DDFA\_V3 [13], HRN3 [11] (3 images) and Era3D [15].

compared against this ground truth. Figure 2 illustrates the implementation of this step in the context of this work.

**High-end facial acquisition.** We built a stereophotogrammetry (SPG) system composed of 10 synchronised DSLR cameras mounted on 5 tripods that were arranged in a semi-circle in two rows at different angles and heights covering on the front and sides of the subject (from 0 to  $\pm 90$  degrees), and two side light sources (Figure 2a) as in [3]. Camera synchronization was crucial to minimize motion artefacts [5]. High-resolution 3D models were subsequently reconstructed and marker-based scaled from the 10 images set of each subject using the Agisoft Metashape software. The resulting 3D facial meshes were manually processed using MeshLab for cleaning, orientation normalization, and facial mesh extraction.

**Low-cost acquisition/reconstruction.** In this work, we applied the methodology to evaluate the following low-cost 3D facial acquisition methods:

- **Mobile phone (MP) scans.** We used Face3DBiomark [18], a client-server architecture that uses an iPhoneX for 3D facial scanning through the TrueDepth infrared camera and a cloud server for mesh processing (Figure 2b). The acquired facial 3D point-cloud was automatically processed with PyMeshLab for facial segmentation, orientation normalisation and remeshing. The acqui-

sition of a facial scan took approximately 15 seconds at a distance of 25-50 cm from the subject.

- **Facial reconstructions from 2D images.** We selected three of the most recent and accurate open-source methods currently available in the literature to reconstruct 3D facial models from 2D images obtained by the SPG system (Figure 2c): 3DDFA\_V3 [13], HRN [11] and Era3D [15]. For 3DDFA\_V3 and Era3D we used a frontal cropped image of dimension 256x256 pixels. In Era3D, background removal was performed to enhance accuracy. For HRN, a multi-view configuration using a frontal and two lateral views was employed, so we refer to the method as HRN3 hereafter. The resulting 3D facial meshes were processed using PyMeshLab for orientation and scale adjustments.

To ensure a fine morphological comparison, all low-cost reconstructions were manually aligned with their high-cost SPG counterparts using MeshLab’s Align Tool, based on five manually selected landmarks (inner eye commissures, nasal septum base, and labial commissure corners). The facial region of all reconstructions was extracted using a 100 mm sphere centered at the nose tip, and Polygon File Format (.PLY) was used for data storage.

### 2.3 Automatic landmarking

The next step of our methodology consists in establishing a standardized landmark-based representation of facial morphology for morphometric evaluations based on GM.

To this end, an automatic and accurate facial landmarking method is required. In this work, 3D facial landmarking was performed by training a 21-landmark multi-view consensus CNN (MV-CNN) model [25] on a proprietary dataset of 125 manually landmarked facial 3D models obtained from SPG scans, distinct from the evaluation dataset. For training hyperparameters, we set a 25-view configuration and the depth channel (*z-buffer*) as the input image modality, following [26].

### 2.4 Evaluation metrics

Our methodology includes evaluation following two complementary approaches: *i*) Geometric analysis —measuring surface accuracy— and *ii*) GM-based morphometric analysis —assessing facial morphology preservation.

**Geometric evaluation metrics.** Point-to-point distance and surface-to-surface deviations are computed by comparing the low-cost reconstructions against their gold-standard equivalents. Since mesh vertex densities differed, point-to-point distances were computed using the nearest neighbour approach via kD-tree search.

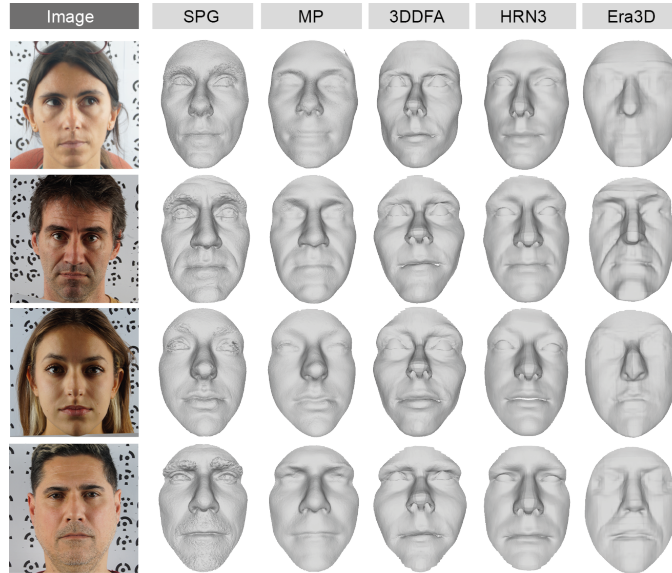


**Fig. 3.** At-a-glance comparison of the geometry of the 3D facial acquisition and reconstruction methods.

***Morphometric evaluation metrics.*** This evaluation comprises quantifying facial morphology using Centroid Size (CS) and Pairwise Procrustes Distances (PPD) morphometrics variables [26], alongside Generalized Procrustes Analysis (GPA) and Euclidean Distance Matrix Analysis (EDMA) for global and local shape characterization.

To apply GPA, we performed Principal Component Analysis (PCA) to visualize global shape variation in morphospace, computing the Intersection-over-Union (IoU) between the convex hulls of high- and low-cost methods and calculated Procrustes Distance (PD) to quantify overall shape differences, with 10,000 permutations for statistical validation.

For EDMA, we analyzed 210 inter-landmark distances, comparing male and female subgroups within each reconstruction method. Using a confidence interval ( $\alpha = 0.10$ ) [24], we identified  $n$  significant inter-landmarks distances. To determine which method best preserved facial morphology, we computed the percentage of *matching distances* (MD, %) by comparing the top-5 ( $n = 5$ ) and top-10 ( $n = 10$ ) longest/shortest inter-landmark distances across methods.

### 3 Results and discussion

***Experimental setup.*** All analysis results and 3D processing of the models have been performed on a Windows PC (16GB RAM with 6-core CPU). 3DDFA\_V3 and HRN3 models were generated on a Linux server (36-core CPU, NVIDIA GeForce RTX 2080 Ti GPUs) and Eras3D models with NVIDIA H100 GPUs pro-

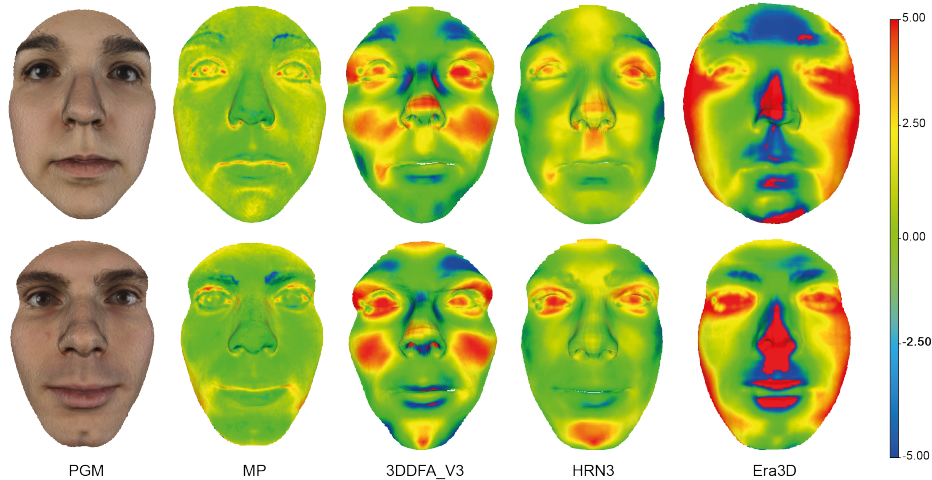


**Fig. 4.** Surface-to-surface deviation between low-cost methods and SPG. Deviation values are coded with a colour map from blue to red.

vided by EuroHPC JU and MareNostrum5 at Barcelona Supercomputing Center. The code implementing all the steps of the methodology, the facial landmarks obtained on each facial model and the MVCNN automatic landmarking model are available at: [https://bitbucket.org/cv\\_her\\_lasalle/gmfacialbenchmark](https://bitbucket.org/cv_her_lasalle/gmfacialbenchmark).

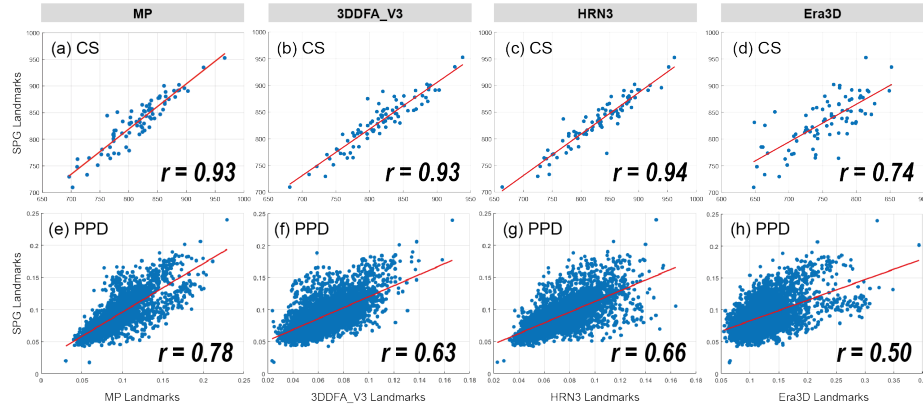
### 3.1 Geometric evaluation

Figure 3 illustrates examples of the 3D facial models obtained from the acquisition and reconstruction methods in our testbed. To focus on geometric accuracy, texture and vertex colours were omitted.

Table 1 shows the point-to-point distances between the low-cost reconstruction methods with respect to SPG. MP is the method that offers the lowest average distance ( $<1\text{mm}$ ). 3DDFA\_V3 and HRN3 show a similar behaviour, with the latter generating a slightly lower error. Era3D is the furthest away from the gold-standard.

**Table 1.** Point-to-point (in mm) average distance  $\pm$  standard deviation (SD) and maximum distance between low-cost methods and SPG.

Method	Avg. Distance $\pm$ SD (mm)	Max. Distance (mm)
MP	$0.96 \pm 0.75$	6.32
3DDFA_V3	$1.91 \pm 1.44$	11.57
HRN3	$1.45 \pm 1.14$	12.16
Era3D	$2.82 \pm 2.32$	12.65



**Fig. 5.** (a-d) Centroid Size (CS) and (e-h) Pairwise Procrustes Distances (PPD) between SPG and low-cost methods. The  $r$  coefficient shows the correlation between variables.

These findings are complemented by the surface-to-surface deviation coded in Figure 4. We observed the loss of high-frequency detail in MP, especially in the commissures of the mouth and eyes. 3DDFA\_V3 showed a large deviation in the area of the nose, cheekbones and eyes. HRN3 preserved eye detail but deviated from SPG, though it improved in the mouth region. Era3D shows a flattening of the facial morphology and a large overall deviation from SPG.

### 3.2 Morphometric evaluation

On the basis of the anatomical landmarks coordinates, the morphometric variables (Figure 5) display the correlation between the CS and PPD computed from the SPG and low-cost methods registered landmarks, portraying the correlation coefficient  $r$  for each comparison. In all cases, the correlations were significant with a  $p$ -value  $< 0.0001$ . For both variables, we found a similar behaviour between the MP, 3DDFA\_V3 and HRN3 methods, while Era3D displayed lower correlation values. In the case of PPD we observed a higher correlation between the landmarks on the SPG and MP models (Figure 5e), which reveals a greater morphological similarity between the two methods.

From the landmark vectors resulting from the GPA, Figure 6 shows the Intersection-over-Union (IoU) between the convex hulls of the high and low-cost groups in the PCA morphospace. The highest value (IoU = 0.62) was observed in the comparison of SPG and MP (Figure 6a), where the convex-hulls are very similar and defined by the same individuals, showing the morphological similarity between methods. The rest of the low-cost reconstructions displayed lower IoU values and very disparate convex hulls, demonstrating large deviations in facial shape from the gold-standard.

These results were accompanied by the Procrustes Distance (PD), where MP has the lowest value (PD = 0.026), followed by HRN3 (PD = 0.033), 3DDFA\_V3

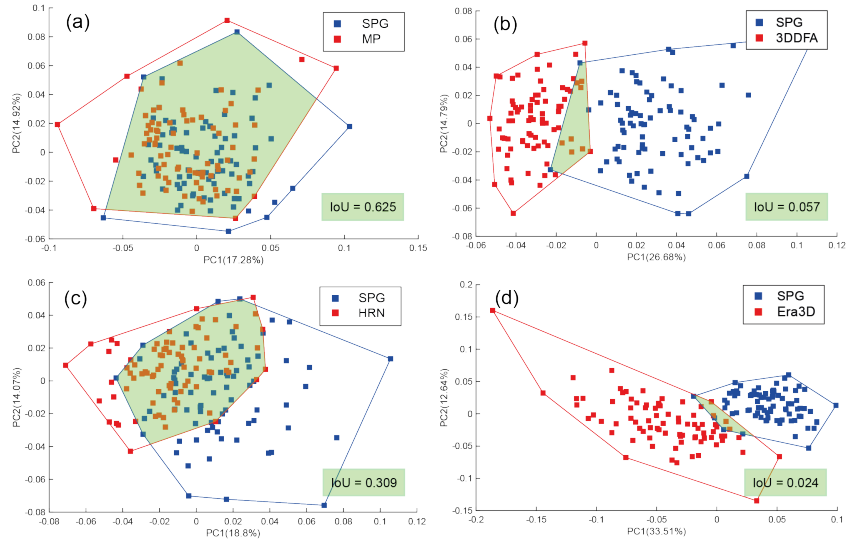


**Fig. 6.** GPA morphospaces comparing SPG with (a) MP, (b) 3DDFA\_V3, (c) HRN3 and (d) Era3D low-cost methods.

(PD = 0.059) and Era3D (PD = 0.091) versus SPG GPA coordinates. However, for all methods, we found significant differences ( $p$ -value < 0.05) between GPA coordinates of SPG and low-cost methods.

Finally, Figure 7 showcases the top-10 most significant shorter and longer inter-landmark distances between male and female groups for each low-cost method. Since the same individuals were used in all methods and no inter-observer landmark variability was introduced, the only variable factor was the acquisition/reconstruction method. This allowed us to directly compare which low-cost method best preserved the facial shape differences observed in the SPG gold-standard.

In the SPG reference case (Figure 7a), the most distinctive differences between males and females were in eye spacing and nose size. While all low-cost methods captured nose size differences, MP (Figure 7b) was the only method to also detect significant variations in eye spacing, making it the most accurate in replicating SPG’s sex-based shape differences. The matching inter-landmark distances across methods are represented as thick dashed lines in Figure 7.

These results are further supported by the matching distances (MD) values in Table 2. In the top-5 comparison, MP achieved a perfect match (100%) with the SPG reference, while the other methods showed lower coincidence. Even in the top-10 analysis, MP maintained the highest percentage of matching distances, reinforcing its higher similarity to SPG in consistency with the previous shape analysis experiments.

**Table 2.** EDMA evaluation of low-cost methods: matching distances (%) between the top-5 and top-10 significant inter-landmark distances.

Top-5								
MP		3DDFA_V3		HRN3		Era3D		
	Longer	Shorter	Longer	Shorter	Longer	Shorter	Longer	Shorter
MD (%)	100	100	40	40	60	40	40	40
Avg. MD (%)	100		40		50		40	
Top-10								
MP		3DDFA_V3		HRN3		Era3D		
	Longer	Shorter	Longer	Shorter	Longer	Shorter	Longer	Shorter
MD (%)	90	50	50	40	50	30	50	40
Avg. MD (%)	70		45		40		45	

## 4 Conclusions

This study has presented a novel methodology for evaluating low-cost 3D facial acquisition and reconstruction methods combining geometric and morphometrics accuracy metrics. By integrating GM-based shape analysis, the proposed methodology provides a statistically robust and biologically meaningful validation framework, offering a more comprehensive assessment of facial morphology preservation.

The methodology has been applied in a case of use comprising stereophotogrammetry as the gold standard, smartphone-based low-cost facial acquisition and deep learning-based 3D facial reconstruction methods from 2D images.

Results demonstrate that smartphone scans show higher accuracy than facial reconstruction methods in terms of geometric and morphometric evaluation metrics. However, although MP showed better performance, its requirement for a static capture process presents practical limitations, which 2D imaging-based methods could overcome despite their slightly lower accuracy. These findings emphasize the need for further advancements in low-cost 3D reconstruction techniques to enhance their precision and reliability for clinical applications. The proposed methodology serves as a valuable tool for guiding these improvements.

## 5 Acknowledgments

We are grateful for the voluntary collaboration of all participants. This research was supported by AGAUR’s Knowledge Industry Programme (2021 LLAV 00044), the Joan Oró grant from the DRU of the Generalitat de Catalunya (2024 FI-3 00160) and the European Social Fund, by the Fundación Álvaro Entrecanales-Lejeune predoctoral grant and by the Agencia Española de Investigación (PID2020-113609RB-C21/AEI/10.13039/501100011033, PID2023-147001OB-C22). We also acknowledge EuroHPC JU for awarding the project ID EHPC-043 access to MareNostrum5 at Barcelona Supercomputing Center and the Agència

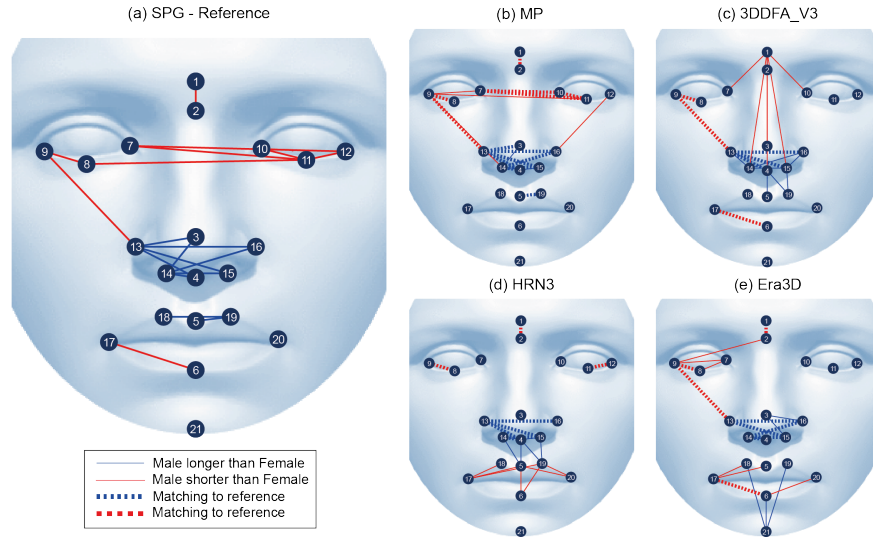


**Fig. 7.** EDMA top-10 significant inter-landmarks distances comparison between males and females for each 3D facial acquisition/reconstruction method: (a) SPG, used as reference, (b) MP, (c) 3DDFA\_V3 (d) HRN3 and (e) Era3D.

de Gestió d’Ajuts Universitaris i de Recerca (AGAUR) of the Generalitat de Catalunya (2021 SGR01396, 2021 SGR00706).

## References

1. Li, Y., Yang, X., Li, D.: The Application of Three-Dimensional Surface Imaging System in Plastic and Reconstructive Surgery. *Annals of Plastic Surgery*. 77, S76 (2016).
2. Sarver, D.M.: Interactions of hard tissues, soft tissues, and growth over time, and their impact on orthodontic diagnosis and treatment planning. *American Journal of Orthodontics and Dentofacial Orthopedics*. 148, 380–386 (2015).
3. Starbuck, J.M., et al.: Green tea extracts containing epigallocatechin-3-gallate modulate facial development in Down syndrome. *Sci Rep*. 11, 4715 (2021).
4. Parsa, S., et al.: Current and Future Photography Techniques in Aesthetic Surgery. *Aesthetic Surgery Journal Open Forum*. 4, ojab050 (2022).
5. Heike, C.L., Upson, K., Stuhaug, E., Weinberg, S.M.: 3D digital stereophotogrammetry: a practical guide to facial image acquisition. *Head & Face Medicine*. 6, 18 (2010).
6. Koban, K.C., et al.: Validation of two handheld devices against a non-portable three-dimensional surface scanner and assessment of potential use for intraoperative facial imaging. *Journal of Plastic, Reconstructive & Aesthetic Surgery*. 73, 141–148 (2020).
7. Li, M., et al.: Rapid automated landmarking for morphometric analysis of three-dimensional facial scans. *J Anat*. 230, 607–618 (2017).
8. Heredia-Lidón, Á., et al.: Automated Orientation Detection of 3D Head Reconstructions from sMRI Using Multiview Orthographic Projections: An Image

- Classification-Based Approach. In: Pertusa, A., Gallego, A.J., Sánchez, J.A., and Domingues, I. (eds.) *Pattern Recognition and Image Analysis*. pp. 603–614. Springer Nature Switzerland, Cham (2023).
9. Gibelli, D., Pucciarelli, V., Cappella, A., Dolci, C., Sforza, C.: Are Portable Stereophotogrammetric Devices Reliable in Facial Imaging? A Validation Study of VECTRA H1 Device. *Journal of Oral and Maxillofacial Surgery*. 76, 1772–1784 (2018).
  10. D’Ettorre, G., et al.: A comparison between stereophotogrammetry and smartphone structured light technology for three-dimensional face scanning. *Angle Orthod.* 92, 358–363 (2022).
  11. Lei, B., Ren, J., Feng, M., Cui, M., Xie, X.: A Hierarchical Representation Network for Accurate and Detailed Face Reconstruction from In-The-Wild Images. Presented at the 2023 IEEE/CVF Conference on Computer Vision and Pattern Recognition (CVPR) June 1 (2023).
  12. Deng, Y., et al.: Accurate 3D Face Reconstruction With Weakly-Supervised Learning: From Single Image to Image Set. In: 2019 IEEE/CVF Conference on Computer Vision and Pattern Recognition Workshops (CVPRW). pp. 285–295 (2019).
  13. Wang, Z., Zhu, X., Zhang, T., Wang, B., Lei, Z.: 3D Face Reconstruction with the Geometric Guidance of Facial Part Segmentation. In: 2024 IEEE/CVF Conference on Computer Vision and Pattern Recognition (CVPR). pp. 1672–1682 (2024).
  14. Ramon, E., et al.: H3D-Net: Few-Shot High-Fidelity 3D Head Reconstruction. In: 2021 IEEE/CVF International Conference on Computer Vision (ICCV). pp. 5600–5609 (2021).
  15. Li, P., et al.: Era3D: High-Resolution Multiview Diffusion using Efficient Row-wise Attention, <http://arxiv.org/abs/2405.11616>, (2024).
  16. Liu, Y., et al.: SyncDreamer: Generating Multiview-consistent Images from a Single-view Image, <http://arxiv.org/abs/2309.03453>, (2024).
  17. Tang, J., et al.: LGM: Large Multi-View Gaussian Model for High-Resolution 3D Content Creation, <http://arxiv.org/abs/2402.05054>, (2024).
  18. Heredia Lidón, Á. et al.: Face3DBiomark: a low-cost solution to compute 3D facial biomarkers for diagnosing conditions with associated facial dysmorphologies. *IEEE International Symposium on Biomedical Imaging (ISBI)*. (2024).
  19. Kazhdan, M., Hoppe, H.: Screened poisson surface reconstruction. *ACM Trans. Graph.* 32, 29:1-29:13 (2013).
  20. Ritschl, L.M., et al.: Comparison of three-dimensional imaging of the nose using three different 3D-photography systems: an observational study. *Head Face Med.* 20, 7 (2024).
  21. Chai, Z., et al.: REALY: Rethinking the Evaluation of 3D Face Reconstruction, <http://arxiv.org/abs/2203.09729>, (2022).
  22. Sanyal, S., et al.: Learning to Regress 3D Face Shape and Expression from an Image without 3D Supervision, <http://arxiv.org/abs/1905.06817>, (2019).
  23. Mitteroecker, P., Gunz, P.: Advances in Geometric Morphometrics. *Evol Biol.* 36, 235–247 (2009).
  24. Lele, S.R., Richtsmeier, J.T.: *An Invariant Approach to Statistical Analysis of Shapes*. Chapman and Hall/CRC, New York (2001).
  25. Paulsen, R.R., et al.: Multi-view consensus CNN for 3D facial landmark placement, (2019).
  26. Heredia-Lidón, Á., et al.: A Critical Comparison Between Template-Based and Architecture-Reused Deep Learning Methods for Generic 3D Landmarking of Anatomical Structures. In: Wachinger, C., Paniagua, B., Elhabian, S., Luijten, G.,

and Egger, J. (eds.) Shape in Medical Imaging. pp. 97–111. Springer Nature Switzerland, Cham (2025).